Adsorption (2009) 15: 114–122
DOI 10.1007/s10450-009-9162-0

Fine pore mouth structure of molecular sieve carbon with GCMC-assisted supercritical gas adsorption analysis

Ryoji Kobori · Tomonori Ohba · Takaomi Suzuki · Taku Iiyama · Sumio Ozeki · Michio Inagaki · Akihiro Nakamura · Masato Kawai · Hirofumi Kanoh · Katsumi Kaneko

Published online: 23 March 2009

Abstract N_2 adsorption isotherms of molecular sieve carbon were measured at 77 K and 303 K. The Ar adsorption isotherms of molecular sieve carbon samples were also measured at 303 K. The grand canonical Monte Carlo (GCMC) simulation technique was applied to calculate the N_2 and Ar adsorption isotherms at 303 K using the ultramicropore volume determined by H_2O adsorption. The comparative method of experimental and simulated isotherms of supercritical N_2 and Ar at 303 K gave the width of the micropore mouth of the molecular sieve carbon, which can be applied to the ultramicropore width determination for other noncrystalline porous solids.

Keywords Molecular sieve carbon · Characterization · Supercritical gas adsorption · GCMC simulation

R. Kobori · T. Ohba (✉) · H. Kanoh · K. Kaneko
Graduate School of Science, Chiba University, 1-33 Yayoi, Inage, Chiba 263-8522, Japan
e-mail: ohba@pchem2.s.chiba-u.ac.jp

T. Suzuki
Department of Environmental Science and Technology, Shinshu University, 4-17-1 Wakasato, Nagano 380-8553, Japan

T. Iiyama · S. Ozeki
Department of Chemistry, Shinshuu University, 3-11 Asahi, Matsumoto, Nagano 390-8621, Japan

M. Inagaki
Department of Applied Chemistry, Aichi Institute of Technology, 1247, Yachigusa, Yakusa, Toyota 470-0392, Japan

A. Nakamura · M. Kawai
Nippon Sanso Co., 3054-3 Shimokurosawa, Takane-Cho, Kitakomagun, Yamanashi 408-0015, Japan

1 Introduction

Green house effect promotes fundamental researches associating with energy saving technologies. Especially, active researches on porous materials have been done from the above aspect all over the world. IUPAC proposed the following classification with pore width w: $w < 2$ nm; micropores ($w < 0.7$ nm; ultramicropores and 0.7 nm $< w <$ 2 nm; supermicropores), 2 nm $< w <$ 50 nm; mesopores, and 50 nm $< w$; macropores. In particular, molecular sieve carbon, which has been used for gas separation, should be one of key materials indispensable to better energy-saving technology. Molecular sieve carbon can be produced from natural products such as nutshells and olive stones with carbonization and special modification treatment (Xu et al. 1996; Nguyen and Do 1995; Braymer et al. 1994; Verma and Walker 1992; Miura and Hayashi 1991). Then development of molecular sieve carbon is in harmony with the preservation of global environment. Thus, the modern technology needs higher performance materials for gas separation. We must design a better molecular sieve carbon with the aid of an accurate evaluation method of the pore size, although the structure is non-crystalline. As a remarkable molecular sieve effect is observed in ultramicroporous carbons, the accurate determination method of the pore width of molecular sieve materials must be given on the basis of molecular science.

Ordinary a variety of molecular sieve carbons are produced by (1) carbonization of special materials at optimum conditions, (2) high temperature treatment of activated carbon, (3) carbon deposition at the pore mouth, (4) film coating of ultramicropore, (5) pore reopening after blocking micropores (Cabrera et al. 1993; Kawabuchi et al. 1996). The optimum method is adopted for each starting material using the selectivity test of gas separation.

The selectivity of gas separation has been believed to come from a match of the pore mouth width for the molecular size. However, the molecular size depends on the microscopic environment in the ultramicropore. We can use several molecular size values determined from the van der Waals constant, bulk liquid density, solid density, in addition to the Lennard-Jones parameters (Avnir et al. 1983; Livingston 1944). These values are variable, depending on the nano-level structure surrounding the probe molecule. Then we must take into account the fact that the molecular size can vary according to the molecule-molecule and molecule-pore wall interactions. This microscopic view should be introduced in understanding of molecular sieve effect.

N_2 adsorption at 77 K has been helpful to determine the pore size distribution (Gregg and Sing 1982; Kaneko 1994). In particular, we can use established evaluation methods using N_2 adsorption isotherm for mesopores, since a fundamental discussion has been done for small mesopores (Dollimore and Heal 1978; Pierce 1953). As to supermicropores, new approaches such as density functional theory method (DFT) and grand canonical Monte Calro (GCMC) simulation are going to succeed to give a reasonable pore size distribution regardless of necessity for further studies (Jagiello and Thommes 2004; Do and Do 2003; Dombrowski et al. 2000; El-Merraoui et al. 2000; Lastoskie et al. 1993a, 1993b; Ravikovitch et al. 2000; Seaton et al. 1989; Cracknell et al. 1995).

However, characterization of ultramicropores is less advanced. Nitrogen molecules are strongly adsorbed on the entrance of the ultramicropore at 77 K, blocking further adsorption. Consequently, N_2 adsorption at 77 K cannot be applied to the molecular sieve carbon. Kaneko et al. have tried to develop He adsorption at 4.2 K, showing that He adsorption at 4.2 K can give a detailed information on the ultramicropore in comparison with N_2 adsorption, but even He adsorption cannot be applied to ultramicropores whose pore width is less than about 0.6 nm (Setoyama and Kaneko 1995; Setoyama et al. 1996; Kuwabara et al. 1991). Multi-molecular probe techniques have been proposed to evaluate the pore size of the molecular sieve carbon. The multi-molecular probe (MMP) technique can be classified into kinetic and equilibrium methods (Carrott 1995; Gonzalez et al. 1997). The equilibrium MMP method can provide the possible zone of the pore width, while the kinetic MMP method gives the possible zone of an apparent pore width under the flow conditions. The adsorption measurement of N_2 from the ultrahigh vacuum range was also introduced; this superwide-pressure range adsorption still not so perfect for ultramicropore characterization (Sunaga et al. 2004). Therefore, we must try to develop the high-resolution determination method of the pore mouth of the molecular sieve carbon to show the fine structure of ultramicropores. An accurate determination of the pore size distribution of ultramicropores should accelerate the development of a high performance molecular sieve carbon. In a preceding letter, GCMC simulation assisted supercritical N_2 gas adsorption (GCMC-GA) analysis for the average pore width determination of molecular sieve carbon was reported (Suzuki et al. 2000). In this article, the detailed procedure and an improved evaluation method using N_2 and Ar adsorption are proposed.

2 GCMC simulation and experimental

2.1 GCMC-assisted supercritical gas adsorption method

The method proposed here is composed of experimental and GCMC simulation studies. As N_2 and Ar molecules are sufficiently adsorbed on molecular sieve carbon even at ambient temperature and subatmospheric pressure, N_2 and Ar adsorption isotherms at 303 K are simulated with GCMC simulation. However, the ultramicropore volume is necessary for fitting of the experimental isotherm to the simulated isotherms. Accordingly the micropore volume is estimated by water adsorption. Although water vapor is not adsorbed on molecular sieve carbon at a low relative pressure (P/P_0) region, water vapor is sufficiently adsorbed above $P/P_0 = 0.6$. Hence this method is available for evaluation of ultramicropores where water molecules are accessible. Iiyama et al. showed that water molecules adsorbed in carbon micropores formed an ordered structure using X-ray diffraction (Iiyama et al. 1995). Hence the mean density of bulk liquid and solid of water was used for evaluation of the ultramicropore volume, although the density difference gives rise to an error. Also Iiyama et al and Ohba et al. studied water structures confined in carbon micropores with in situ small angle X-ray scattering; they showed that small angle X-ray scattering intensity of water adsorbed activated carbon fiber of predominant ultramicropores became slight near the saturated vapor pressure, indicating almost complete filling of ultramicropores with water (Iiyama et al. 1995, 1997; Ohba et al. 2004, 2005). Then, we assumed that water vapors were adsorbed in ultramicropores and the pore volume determined by water adsorption was used for comparison of experimental adsorption isotherms of N_2 and Ar with the simulated adsorption isotherms.

The intermolecular interaction between gas molecules is approximated by the one-center Lennard-Jones potential.

$$\phi_{ij}(r) = 4\varepsilon_{ff}\left[\left(\frac{\sigma_{ff}}{r_{ij}}\right)^{12} - \left(\frac{\sigma_{ff}}{r_{ij}}\right)^{6}\right]. \quad (1)$$

Here ε_{ff} and σ_{ff} are the intermolecular potential well depth and the contact diameter; $\varepsilon_{ff}/k_B = 104.2$ K and $\sigma_{ff} = 0.3632$ nm for N_2 and $\varepsilon_{ff}/k_B = 141.6$ K and $\varepsilon_{ff} =$

0.3350 nm for Ar, and r_{ij} is the intermolecular distance. The interaction potential $\varepsilon_{sf}(z)$ of a molecule with a single graphite slab is described by the Steele's 10-4-3 potential function

$$\phi_{sf}(z) = A\left[\frac{2}{5}\left(\frac{\sigma_{sf}}{z}\right)^{10} - \left(\frac{\sigma_{sf}}{z}\right)^{4} - \frac{\sigma_{sf}^4}{3\Delta_C(z+0.61\Delta_C)^3}\right], \tag{2}$$

where A is $2\pi\sigma_{sf}^2\varepsilon_{sf}\rho\Delta_C$, z is the vertical distance of the molecule from a graphite surface layer, ρ is the carbon atomic number, Δ_C is the interlayer distance, and ε_{sf} and σ_{sf} are fitted parameters of the molecule-carbon potential well depth and the effective diameter, respectively (Steele 1973). Values of 54.3 K for ε_{sf}/k and 0.353 nm for σ_{sf} were obtained for the N_2-carbon system with the use of the Lorentz-Berthelot rules ($\varepsilon_{sf}/k = 63.2$ K and $\sigma_{sf} = 0.339$ nm for the Ar-carbon system). The interaction potential between the graphite pore and an adsorbate molecule is given as

$$\Phi = \phi_{sf}(H - z) + \phi_{sf}(z) \tag{3}$$

for the slit system of a physical width H. We used a periodic boundary condition for the slit-shaped unit cell in the x and y directions (Allen and Tildesley 1988). The cell size was $l \times l \times w$, where l and w are the length and slit width, respectively. Here the slit width w is not equal to the physical width of H, which is determined as the distance between opposite carbon atom layers, but w is the empirical pore width, which is determined by the molecular adsorption experiment. The empirical pore width w was approximated by (4) (Kaneko et al. 1994).

$$W = H - 2 \times 0.856\sigma_{sf} + \sigma_{ff}. \tag{4}$$

The above GCMC calculation of the adsorption isotherm at 303 K was carried out for the graphite-slit model for $w = 0.40 - 0.65$ nm and $l = 6$ nm (Ohba et al. 2003). The pressure P for a chemical potential was directly calculated from the molecular density using GCMC simulation without the wall potential.

2.2 Measurement of N_2, Ar, and H_2O adsorption

N_2 adsorption isotherms were gravimetrically measured at 77 K and 303 K. The N_2 adsorption isotherm at 77 K was used for evaluation of the average pore width. Ar adsorption isotherms were also measured gravimetrically at 303 K for necessary samples. Water adsorption isotherms were measured at 303 K. Samples were evacuated at 523 K and <10 mPa for 2 h prior to the adsorption measurement.

Five kinds of molecular sieve carbon samples and activated carbon fiber (ACF, $w = 0.7$ nm) were used. Samples are named as MSC-A, -B, -C, -D, -E, and ACF. Here, MSC-A and -B are MSC-5A and MSC-3A (Takeda Co.), respectively. MSC-C was supplied by Nihon Sanso Co., while MSC-D and -E were supplied by M. Inagaki. ACF is pitch-based activated carbon fiber, which was supplied by ADALL Co.

The ultramicropore volumes of MSC-A, -B, and -C were determined by the following water adsorption measurement (Zsigmondy et al. 1912; Lide 1992–1993) The sample was dried at 523 K in a flow of helium gas (50 ml min^{-1}) for 2 h and granular samples of A, B, and C were immersed in distilled water for 3 days at 303 K. In case of powdered samples of D and E and ACF, they were kept under the saturated vapor pressure for 3 days at 303 K. After the replacement of air in ultramicropores with water, the sample was kept at 303 K under the relative humidity of 93% for more than 40 h using saturated KNO_3 solution in order to remove liquid water on the external surface of the sample. The mass difference between under the 93% relative humidity and after drying was regarded as the saturated amount of water adsorption. The reliability of this replacement method was checked for MSC-A, B, and C; the saturated adsorption amounts of these three samples determined by the representative gravimetric method using a vacuum line coincided with those from the replacement method within 7%.

3 Results and discussion

3.1 Evaluation of ultramicropore volume

Figure 1 shows adsorption isotherms of water on MSC-A, -B, and -C at 303 K. All isotherms have almost no adsorption hysteresis, although the adsorption isotherm of water

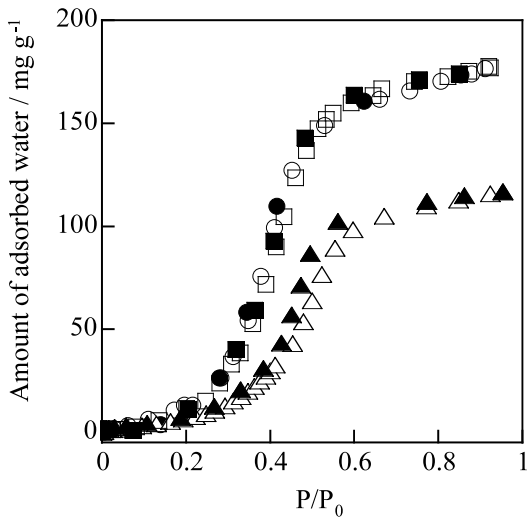

Fig. 1 Water adsorption and desorption isotherms on MSCs at 303 K. (○, ●); MSC-A, (△, ▲); MSC-B, and (□, ■); MSC-C. *Open* and *solid symbols* denote adsorption and desorption branches, respectively

Table 1 The pore volume of MSCs from the amount of water adsorption at 303 K and α_S-plot analysis of N_2 adsorption isotherms at 77 K

Sample	Water replacement method /ml g^{-1}	N_2 adsorption at 77 K /ml g^{-1}
MSC-A	0.176	0.186
MSC-B	0.133	
MSC-C	0.181	
MSC-D	0.149	0.188
MSC-E	0.186	
ACF	0.241	0.312

on ordinary activated carbon of supermicropores has a clear hysteresis. However, activated carbon of low burn-off has no hysteresis in the water adsorption isotherm as well as these molecular sieve carbon samples (Carrott et al. 1991; Kaneko et al. 1999). The low burn-off activated carbon has the average micropore width less than 0.7–0.8 nm according to the high resolution α_S-analysis (Kaneko et al. 1999). Hence, the absence of the adsorption hysteresis in the water adsorption isotherm suggests the micropore width less than 0.8 nm. MSC-A has meaningful amounts of water adsorption even below $P/P_0 = 0.3$, whereas almost no water molecules are adsorbed on MSC-B below $P/P_0 = 0.3$.

The abrupt rising in the water adsorption isotherm at $P/P_0 = 0.3 \sim 0.4$ should be associated with the formation of the unit cluster of water molecules (Kaneko et al. 1998). Iiyama et al. and Ohba et al. have studied the structure of cluster and formation process of the cluster in micropores of activated carbon fiber (ACF) by use of *in situ* X-ray diffraction, *in situ* small angle X-ray scattering, and GCMC simulation, indicating that the cluster structure and formation process depend on the pore width (Iiyama et al. 1995, 1997; Ohba et al. 2004, 2005). However, the mechanism of water adsorption on activated carbon is not fully elucidated. In particular, water adsorption mechanism on molecular sieve carbon is a future research subject. Here, the saturated amount of water adsorption was compared with that determined from the water replacement method. The saturated amount of water adsorption at $P/P_0 = 1$ which is determined by the extrapolation, is 180 mg g^{-1} for MSC-A, 120 mg g^{-1} for MSC-B, and 180 mg g^{-1} for MSC-C. The saturated amounts of water adsorption from the water replacement method are 168±3 mg g^{-1} for MSC-A, 127±5 mg g^{-1} for MSC-B, and 173±5 mg g^{-1} for MSC-C. Hence these volumes determined by different methods coincide with each other within 8% of the maximum error.

The ultramicropore volume determined by the water replacement method at 303 K is listed on Table 1. Here the ultramicropore volume was obtained using the mean value of the bulk liquid density at 303 K (0.995 g ml^{-1}) and bulk solid density at 273 K (0.918 g ml^{-1}), although the difference of the ultramicropore volumes calculated from both

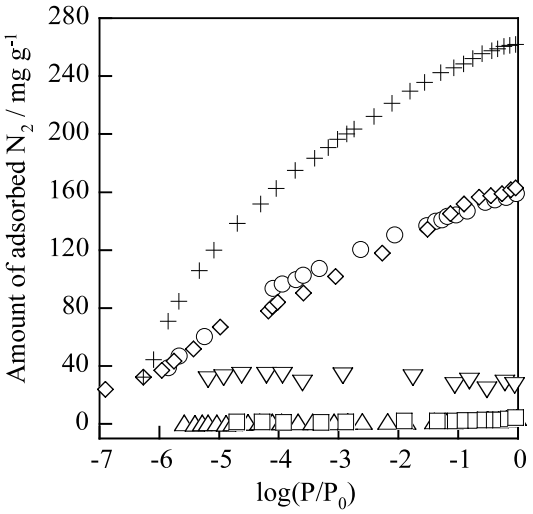

Fig. 2 N_2 adsorption and desorption isotherms on MSCs and ACF at 77 K. (○); MSC-A, (△); MSC-B, (□); MSC-C, (◇); MSC-D, (▽); MSC-E, and (+); ACF

density values is less than 10%. The *in situ* X-ray diffraction study mentioned above showed that the structure of water adsorbed in micropores of ACF ($w = 0.7$ nm) is highly ordered compared with that of bulk liquid and water adsorbed in the micropores has no DSC peak for melted water (Iiyama et al. 1995, 1997; Kaneko et al. 1992). Then the mean density of solid and liquid was used.

In the case of MSC-A and -D and ACF, the adsorption isotherms of N_2 at 77 K were measured, as shown in Fig. 2. The abscissa of the adsorption isotherm is expressed by the logarithm of P/P_0. The adsorption isotherms of MSC-A, -D, and -E rise even below $P/P_0 = 10^{-3}$, being characteristics of micropore filling. The amount of N_2 adsorption on MSC-E at 77 K is greater than 20 mg g^{-1}, while those of other two samples of MSC-B and -C are less than 5 mg g^{-1}. In the case of the latter two samples (MSC-B and -C), a serious pore blocking should occur, suggesting that pore width of both samples is smaller than that of other samples. The adsorption isotherms of N_2 on MSC-A and -D and ACF at 77 K were analyzed by α_S-plot, as shown in Fig. 3. Setoyama et al. showed that α_S-plot has a predominant upward swing from the linear increase below $\alpha_S = 0.5$ for molecular sieve carbon of $w < 0.8$ nm using the GCMC simulation (Setoyama et al. 1998). The observed α_S-plot agrees with that predicted by the above simulation. The surface area, micropore volume, and average pore width can be evaluated from the linear plot passing both of the origin and the point at $\alpha_S = 0.5$ within 15% of the error regardless of the upward swing. Here, the density of liquid N_2 (0.808 g ml^{-1}) was used for the evaluation of the micropore volume.

The micropore volume obtained from N_2 adsorption at 77 K is also listed in Table 1. The micropore volumes of MSC-A and -D and ACF from N_2 adsorption are greater

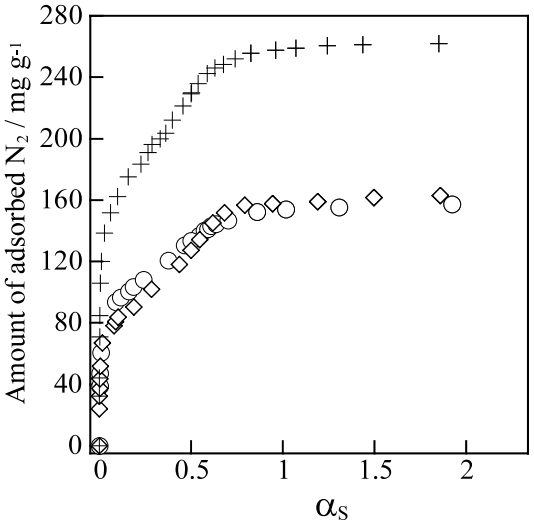

Fig. 3 α_S-plot of N_2 adsorption and desorption isotherms at 77 K. (○); MSC-A, (◇); MSC-D, and (+); ACF

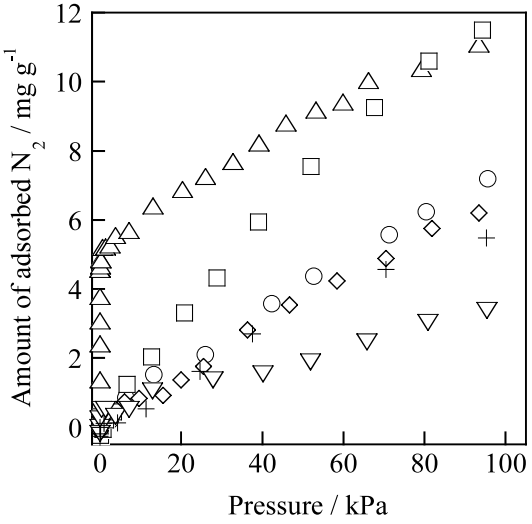

Fig. 4 N_2 adsorption and desorption isotherms on MSCs and ACF at 303 K. (○); MSC-A, (△); MSC-B, (□); MSC-C, (◇); MSC-D, (▽); MSC-E, and (+); ACF

Table 2 Pore structural parameters of MSC-A, MSC-D, and ACF

Sample	a_t /m^2 g^{-1}	a_{ext} /m^2 g^{-1}	V /ml g^{-1}	w /nm
MSC-A	539	5	0.186	0.69
MSC-D	540	13	0.188	0.71
ACF	973	13	0.312	0.65

than those from the water replacement method. As the N_2 adsorbed layer in ultramicropores has a denser structure than the bulk liquid N_2, the micropore volume from N_2 adsorption should be overestimated. Table 2 shows the total surface area a_t, external surface area a_{ext}, the micropore volume V, and w. Three samples have almost similar micropore width, being the border width between ultramicropores and supermicropores. The microporous structure parameters from the α_S-plot for other three samples are not shown because of the insufficient N_2 adsorption at 77 K by the serious pore blocking.

3.2 Observed adsorption isotherms of supercritical N_2

The above adsorption isotherms of N_2 at 77 K indicated that the w values of MSC-B, -C, and -E should be less than 0.7 nm. However, the adsorption property for supercritical gas is completely different from that for vapor. That is, the sample of smaller pores can adsorb greater amount of molecules above the critical temperature of N_2 gas. Figure 4 shows adsorption isotherms of supercritical N_2 at 303 K. Basically the amount of N_2 adsorption almost linearly increases with the pressure. Strictly speaking, the relationship is not linear, but slightly convex. Only MSC-B has an unusual uptake at an extremely low pressure, which cannot be

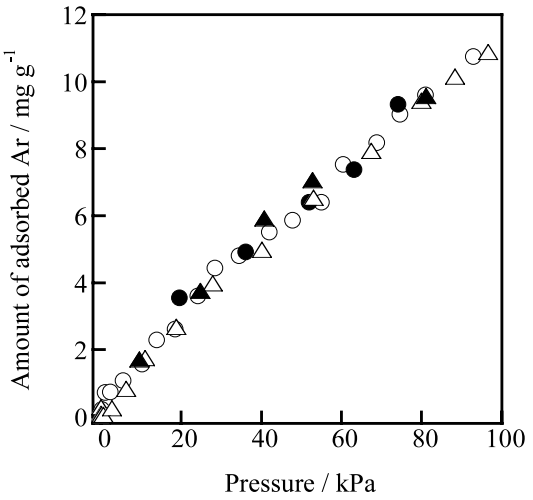

Fig. 5 Adsorption and desorption isotherms of Ar on MSC-A and MSC-B at 303 K. (○, ●); MSC-A, and (△, ▲); MSC-B. *Open* and *solid symbols* indicate adsorption and desorption branches, respectively

desorbed by evacuation at 303 K. Hence, this irreversible adsorption of N_2 suggests the very strong adsorption sites on MSC-B. Figure 5 shows adsorption isotherms of Ar on MSC-A and -B at 303 K. Accidentally both isotherms are almost overlapped each other and no hysteresis. The Ar adsorption isotherm of MSC-B has no initial uptake, as observed in the N_2 adsorption isotherm. Although the structural reason for the strong sites on MSC-B is not understood, we remove the contribution due to the strong sites by a simple subtraction for further discussion. This is because only adsorption in ultramicropores due to the dispersion interaction is considered in the following GCMC-simulation.

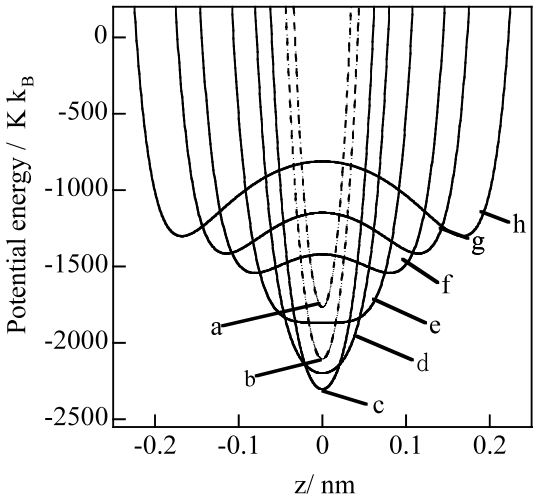

Fig. 6 Potential profile of an N_2 molecule in graphite slit pore as a function of pore width w. (**a**) 0.40 nm; (**b**) 0.42 nm; (**c**) 0.46 nm; (**d**) 0.50 nm; (**e**) 0.56 nm; (**f**) 0.64 nm; (**g**) 0.70 nm; and (**h**) 0.80 nm

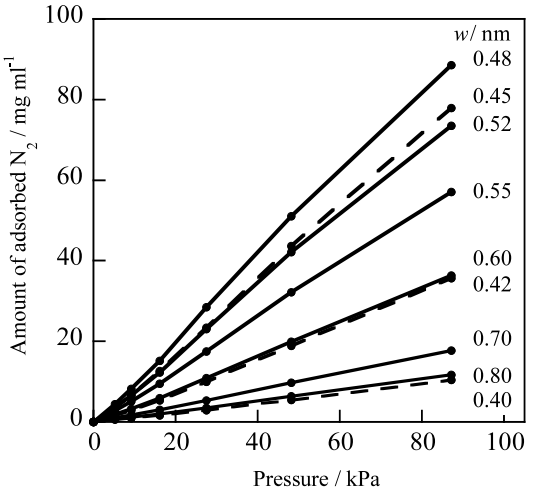

Fig. 7 GCMC simulated N_2 adsorption isotherms at 303 K as a function of pore width w

3.3 Simulated adsorption isotherms of supercritical N_2

The potential profile of an N_2 molecule with the graphite-slit pore provides a whole insight to N_2 adsorption. Figure 6 shows the potential profile of an N_2 molecule as a function of the pore width. Here the center of the abscissa corresponds to the central plane in the slit pore. The potential has a minimum value at the center of the pore ($z = 0$) for $w \leqq 0.56$ nm; the potential well is the deepest for $w = 0.46$ nm whereas the minimum position shifts to the pore walls for $w > 0.63$ nm. The micropore of 0.70 nm has the double minima at the contact position with the pore walls. Although N_2 molecules can be adsorbed on both pore walls $w \geqq 0.70$ nm, the adsorption amount at 303 K should be quite small due to the shallow potential depth. Figure 7 shows the simulated N_2 adsorption isotherms for different pore widths. The simulated adsorption isotherms of supercritical N_2 in the slit graphite pore at 303 K reflect the above interaction potential. The graphite micropore of $w = 0.48$ nm has the greatest adsorption; $w = 0.48$ nm is the critical pore width. In the pore width range of 0.48 to 0.70 nm, the smaller the pore width, the greater the amount of N_2 adsorption. In the case of $w < 0.48$ nm the amount of N_2 adsorption steeply decreases with decrease of w due to the strong repulsive interaction. These simulated N_2 adsorption isotherms are almost linear, but slightly deviate upward, agreeing with the experimental isotherms.

3.4 Comparison of simulated N_2 and Ar isotherms with experimental results

Figure 8 shows both of experimental and simulated N_2 adsorption isotherms at 303 K. The shape of the experimental isotherms is very close to that of the simulated isotherm of

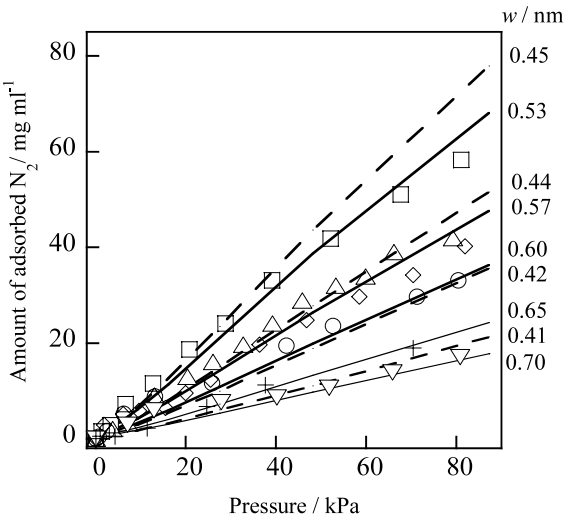

Fig. 8 Comparison of experimental N_2 adsorption isotherms with simulated ones at 303 K. (○); MSC-A, (△); MSC-B, (□); MSC-C, (◇); MSC-D, (▽); MSC-E, and (+); ACF

the specific pore width. Hence, the pore width distribution of the molecular sieve carbon should be quite sharp. Probably N_2 molecules are adsorbed only in the pore mouth which has the deepest potential well. Hence the comparison provides the pore width in which supercritical N_2 can be adsorbed. Figure 9 shows the simulated Ar adsorption isotherms of different pore widths. The simulated Ar isotherms are very similar to the simulated N_2 isotherms in Fig. 7. However, the amounts of adsorption are different from each other. The comparison of the simulated and experimental Ar adsorption isotherms is also shown in Fig. 9. The experimental adsorption isotherm almost coincides with one of simulated isotherms. Consequently, we can determine the pore width of the sample from this comparison.

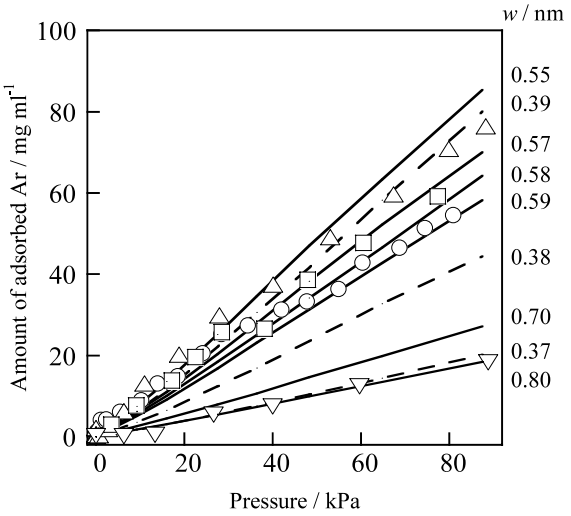

Fig. 9 Comparison of experimental Ar adsorption isotherms with simulated ones at 303 K. (○); MSC-A, (△); MSC-B, (□); MSC-C, (▽); MSC-E

Table 3 Ultramicropore widths of MSC samples and ACF: Here w_{N2} and w_{Ar} are the pore widths from N_2 and Ar adsorptions at 303 K, respectively; w_{α_s} is the pore width from N_2 adsorption at 77 K using α_S-plot

Sample	w_{N_2}/nm	w_{Ar}/nm	w_{α_s}/nm
MSC-A	0.61	0.59	0.69
MSC-B	0.43	0.39	–
MSC-C	0.44	0.39	–
MSC-D	0.59	–	0.71
MSC-E	0.41	0.37	–
ACF	0.65	–	0.65

Fig. 10 Pore structure model of MSC

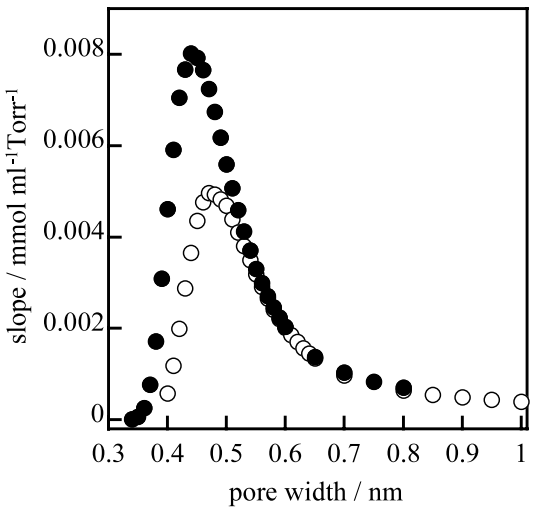

Fig. 11 The relationships between the initial slope of the simulated isotherm and the pore width. (○); N_2 and (●); Ar

3.5 Fine structure of pore mouth

Table 3 shows the ultramicropore width determined by this GCMC-assisted supercritical gas adsorption (GCMC-GA). As the N_2 adsorption isotherms of MSC-A and -D and ACF were measurable even at 77 K, the average pore width from α_S-plot is also shown in Table 3.

The evaluated w values by this GCMC-GA analysis with N_2 are in the range of 0.41 to 0.65 nm, corresponding to the adsorbed N_2 layer range of 1.17 to 1.86. The determined w is reasonable for the molecular sieve effect. The differences of the w from the α_S-plot for MSC-A and -D are 0.08 and 0.12 nm, respectively, which should provide important information on the pore structure. The N_2 adsorption at 77 K can lead to the average pore width of accessible pores for an N_2 molecule. The amount of N_2 adsorption at 77 K is much greater than that at 303 K. Hence, MSC-A and -D should have narrower pore mouth structures whose width is smaller than the average pore width. On the other hand, both determined w values for ACF are identical. Thus, this indicates that the pore entrance size of ACF is the same as that of the deeper pore sites. The average pore width of the inner pores should be greater than the pore width at the pore mouth by the observed difference, as shown in Fig. 10. Here the model of the pore walls compose of five disordered graphitic sheets and the width of the pore mouth is slightly narrower than that of the average value of the inner pore. The w evaluated with GCMC-GA method depends on the probe molecule, as shown in Table 3. The w evaluated with the GCMC-GA method with Ar is slightly smaller than that with N_2. The LJ parameter σ for Ar is smaller than that for N_2. Hence, more Ar molecules can be adsorbed in smaller pores compared with N_2 molecules from the simulated isotherms. Figure 11 shows the changes of the slope of the simulated adsorption isotherm at the origin with the pore width w for N_2 and Ar. Both relations for N_2 and Ar are very close to each other, although for Ar shifts toward a smaller pore width. However, the experimental results in Table 4 request a more careful consideration. The observed fractional filling at 93.1 kPa for N_2 is greater than that for Ar. Here the fractional

Table 4 The experimental fractional filling for N_2 and Ar adsorption at 303 K and 93.1 kPa

Sample	N_2	Ar
MSC-A	0.051	0.046
MSC-B	0.082	0.060
MSC-C	0.084	0.052
MSC-E	0.032	0.015

filling was calculated using the bulk liquid density of N_2 or Ar (N_2: 0.808 g ml^{-1} and Ar: 1.37 g ml^{-1}). The molecular simulation study suggested that the adsorbed density of N_2 in micropores is greater than the bulk liquid density by more than 10%. On the other hand, Ar has no specific interaction other than dispersion interaction and the adsorbed density of Ar is closer to the bulk liquid compared with the observed N_2. Hence, the calculated fractional filling for N_2 may be smaller than the value in Table 4. The fractional filling difference between N_2 and Ar should not be important. The possibility for the fractional filling difference is associated with the spherical approximation for an N_2 molecule. The real N_2 molecule has an oval shape whose short axis is 0.33 nm, being smaller than σ for Ar by 0.01 nm. Accordingly, N_2 molecules can be adsorbed in smaller pores, which is inaccessible for an Ar molecule. In this case, the pore width from N_2 must be overestimated. Therefore we can use the average value between the estimated pore widths from N_2 and Ar adsorption as the pore width of the pore mouth.

In the preceding studies on molecular sieve effect, the matching of the pore geometry with the molecular structure has been stressed. Of course there are not erroneous approaches. However, the concept of the pore width originates from the repulsive interaction in the interaction of a molecule with the pore walls. The attractive interaction inherent to each molecule should be taken into account in order to understand the molecular sieve effect. This study showed the importance of the molecular scientific approach. Also we need to apply quantum molecular sieving effect to evaluate the pore mouth structure of molecular sieving carbon in future (Beenakker et al. 1995; Kumar et al. 2007; Noguchi et al. 2008; Tanaka et al. 2005; Wang et al. 1999).

Acknowledgements Grant-in-Aid for Scientific Research (S) (No. 15101003) by JSPS supported this work.

References

Allen, M.P., Tildesley, D.J.: Computer Simulation of Liquids. Oxford University Press, London (1988). pp. 110

Avnir, D., Farin, D., Pfeifer, P.: Chemistry in noninteger dimensions between two and three. II. Fractal surfaces of adsorbents. J. Chem. Phys. **79**, 3566–3571 (1983)

Beenakker, J.J.M., Borman, V.D., Krylov, S.Y.: Molecular transport in subnanometer pores: zero-point energy, reduced dimensionality and quantum sieving. Chem. Phys. Lett. **232**, 379–382 (1995)

Braymer, T.A., Coe, C.G., Farris, T.S., Gaffney, T.R., Schork, J.M., Armor, J.N.: Granular carbon molecular sieves. Carbon **32**, 445–452 (1994)

Cabrera, A.L., Zellner, J.F., Coe, C.G., Gaffney, T.R., Farris, T.S., Armor, J.N.: Preparation of carbon molecular sieves, I. Two-step hydrocarbon deposition with a single hydrocarbon. Carbon **31**, 969–976 (1993)

Carrott, P.J.M.: Molecular sieve behaviour of activated carbons. Carbon **33**, 1307–1312 (1995)

Carrott, P.J.M., Kenny, M.B., Roberts, R.A., Sing, K.S.W., Theocharis, C.R.: Adsorption of water vapor by microporous solids. Stud. Surf. Sci. Catal. **62**, 685–692 (1991)

Cracknell, R.F., Gubbins, K.E., Maddox, M., Nicholsoisp, D.: Modeling fluid behavior in well-characterized porous materials. Acc. Chem. Res. **28**, 281–287 (1995)

Do, D.D., Do, H.D.: Pore characterization of carbonaceous materials by DFT and GCMC simulations: A review. Ads. Sci. Tech. **25**, 389–423 (2003)

Dollimore, D., Heal, G.R.: The analysis of gas adsorption data to determine pore structure. Surf. Tech. **6**, 231–258 (1978)

Dombrowski, R.J., Hyduke, D.R., Lastoskie, C.M.: Pore size analysis of activated carbons from argon and nitrogen porosimetry using density functional theory. Langmuir **16**, 5041–5050 (2000)

El-Merraoui, M., Aoshima, M., Kaneko, K.: Micropore size distribution of activated carbon fiber using the density functional theory and other methods. Lagmuir **16**, 4300–4304 (2000)

Gonzalez, J.C., Sepulveda-Escribano, A., Molina-Sabio, M., Rodriguez-Reinoso, F.: Characterization of Porous Solid IV. R. Soc. Chem., Lond. (1997)

Gregg, S.J., Sing, K.S.W.: Adsorption, Surface Area and Porosity. Academic Press, New York (1982). pp. 195

Iiyama, T., Nishikawa, K., Otowa, T., Kaneko, K.: An ordered water molecular assembly structure in a slit-shaped carbon nanospace. J. Phys. Chem. **99**, 10075–10076 (1995)

Iiyama, T., Nishikawa, K., Suzuki, T., Kaneko, K.: Study of the structure of a water molecular assembly in a hydrophobic nonospace at low temperature with in situ X-ray diffraction. Chem. Phys. Lett. **274**, 152–158 (1997)

Jagiello, J., Thommes, M.: Comparison of DFT characterization methods based on N_2, Ar, and CO_2 adsorption applied to carbons with various pore size distributions. Carbon **42**, 1277–1232 (2004)

Kaneko, K.: Determination of pore size and pore size distribution 1. Adsorbents and catalysts. J. Membr. Sci. **96**, 59–89 (1994)

Kaneko, K., Ishii, C., Ruike, M., Kuwabara, H.: Origin of superhigh surface area and microcrystalline graphitic structures of activated carbons. Carbon **30**, 1075–1088 (1992)

Kaneko, K., Cracknell, R.F., Nicholson, D.: Nitrogen adsorption in slit pores at ambient temperatures: comparison of simulation and experiment. Langmuir **10**, 4606–4609 (1994)

Kaneko, K., Miyawaki, J., Watanabe, A., Suzuki, T.: Fundamental of Adsorption, 6th edn. Elsevier, Amsterdam (1998). pp. 51

Kaneko, K., Hanzawa, Y., Iiyama, T., Kanda, T., Suzuki, T.: Cluster-mediated water adsorption on carbon nanopores. Adsorption **5**, 7–13 (1999)

Kawabuchi, Y., Kishino, M., Kawano, S., Whitehurst, D.D., Mochida, I.: Carbon deposition from benzene and cyclohexane onto active carbon fiber to control its pore size. Langmuir **12**, 4281–4285 (1996)

Kumar, A.V.A., Jobic, H., Bhatia, S.K.: Quantum effect induced kinetic molecular sieving of hydrogen and deuterium in microporous materials. Adsorption **13**, 501–508 (2007)

Kuwabara, H., Suzuki, T., Kaneko, K.: Ultramicropores in microporous carbon fibres evidenced by helium adsorption at 4.2 K. J. Chem. Soc. Faraday Trans. **87**, 1915–1916 (1991)

Lastoskie, C., Gubbins, K.E., Quirke, N.: Pore size distribution analysis of microporous carbons: A density functional theory approach. J. Phys. Chem. **97**, 4786–4796 (1993a)

Lastoskie, C., Gubbins, K.E., Quirke, N.: Pore size heterogeneity and the carbon slit pore: A density functional theory model. Langmuir **9**, 2693–2702 (1993b)

Lide, D.R. (ed.): Constant humidity solutions. In: Handbook of Chemistry and Physics, pp. 15–20. CRC Press, Boca Raton (1992–1993)

Livingston, H.K.: Cross-sectional areas of molecules adsorbed on solid surfaces. J. Am. Chem. Soc. **66**, 569–573 (1944)

Miura, K., Hayashi, J.: Production of molecular sieving carbon through carbonization of coal modified by organic additives. Carbon **29**, 653–660 (1991)

Nguyen, C., Do, D.D.: Preparation of carbon molecular sieves from macadamia nut shells. Carbon **33**, 1717–1725 (1995)

Noguchi, D., Tanaka, H., Kondo, A., Kajiro, H., Noguchi, H., Ohba, T., Kanoh, H., Kaneko, K.: Quantum sieving effect of three-dimensional Cu-based organic framework for H_2 and D_2. J. Am. Chem. Soc. **130**, 6367–6372 (2008)

Ohba, T., Nicholson, D., Kaneko, K.: Temperature dependence of micropore filling of N_2 in slit-shaped carbon micropores: experiment and grand canonical Monte Carlo simulation. Langmuir **19**, 5700–5707 (2003)

Ohba, T., Kanoh, H., Kaneko, K.: Cluster-growth-induced water adsorption in hydrophobic carbon nanopores. J. Phys. Chem. B **108**, 14964–14969 (2004)

Ohba, T., Kanoh, H., Kaneko, K.: Water cluster growth in hydrophobic solid nanospaces. Chem. Eur. J. **11**, 4890–4894 (2005)

Pierce, C.: Computation of pore sizes from physical adsorption data. J. Phys. Chem. **57**, 149–152 (1953)

Ravikovitch, P.I., Vishnyakov, A., Russo, R., Neimark, A.V.: Unified approach to pore size characterization of microporous carbonaceous materials from N_2, Ar, and CO_2 adsorption isotherms. Langmuir **16**, 2311–2320 (2000)

Seaton, N.A., Walton, J.P.R.B., Quirke, N.: New analysis method for the determination of the pore size distribution of porous carbons from nitrogen adsorption measurements. Carbon **27**, 853–861 (1989)

Setoyama, N., Kaneko, K.: Density of He adsorbed in micropores at 4.2 K. Adsorption **1**, 165–173 (1995)

Setoyama, N., Kaneko, K., Rodriguez-Reinoso, F.: Ultramicropore characterization of microporous carbons by low-temperature helium adsorption. J. Phys. Chem. **100**, 10331–10336 (1996)

Setoyama, N., Suzuki, T., Kaneko, K.: Simulation study on the relationship between a high resolution αs-plot and the pore size distribution for activated carbon. Carbon **36**, 1459–1467 (1998)

Steele, W.A.: Physical interaction of gases with crystalline solids. I. Gas-solid energies and properties of isolated adsorbed atoms. Surf. Sci. **38**, 317–352 (1973)

Sunaga, M., Ohba, T., Suzuki, T., Kanoh, H., Hagiwara, S., Kaneko, K.: Nanostructure characterization of carbon materials with superwide pressure adsorption technique with the aid of grand canonical Monte Carlo simulation. J. Phys. Chem. B **108**, 10651–10658 (2004)

Suzuki, T., Kobori, R., Kaneko, K.: Grand canonical Monte Carlo simulation-assisted pore-width determination of molecular sieve carbons by use of ambient temperature N_2 adsorption. Carbon **38**, 630–633 (2000)

Tanaka, H., Kanoh, H., Yudasaka, M., Iijima, S., Kaneko, K.: Quantum effects on hydrogen isotope adsorption on single-wall carbon nanohorns. J. Am. Chem. Soc. **127**, 7511–7516 (2005)

Verma, S.K., Walker, P.L.: Carbon molecular sieves with stable hydrophobic surfaces. Carbon **30**, 837–844 (1992)

Wang, Q., Challa, S.R., Sholl, D.S., Johnson, K.J.: Quantum sieving in carbon nanoubes and zeolites. Phys. Rev. Lett. **82**, 956–959 (1999)

Xu, S., Guo, S., Jiang, S.: Carbon molecular sieves from walnut shell. Fuel Sci. Tech. Int. **14**, 1447–1459 (1996)

Zsigmondy, R., Bachamann, W., Stevenson, E.F.: Über einen Apparent zur Bestimmung der Dampfspannungs isothermen des Gels der Kieselsäure. Z. anorg. allgem. Chem. **75**, 189–197 (1912)